International Journal of Thermophysics, Vol. 27, No. 4, July 2006 (© 2006)
DOI: 10.1007/s10765-006-0106-6

Vacuum Insulation Panels – Exciting Thermal Properties and Most Challenging Applications[1]

J. Fricke,[2,3] H. Schwab,[2] and U. Heinemann[2]

Vacuum insulation panels (VIPs) have a thermal resistance that is about a factor of 10 higher than that of equally thick conventional polystyrene boards. VIPs nowadays mostly consist of a load-bearing kernel of fumed silica. The kernel is evacuated to below 1 mbar and sealed in a high-barrier laminate, which consists of several layers of Al-coated polyethylene (PE) or polyethylene terephthalate (PET). The laminate is optimized for extremely low leakage rates for air and moisture and thus for a long service life, which is required especially for building applications. The evacuated kernel has a thermal conductivity of about 4×10^{-3} $W \cdot m^{-1} \cdot K^{-1}$ at room temperature, which results mainly from solid thermal conduction along the tenuous silica backbone. A U-value of $0.2\,W \cdot m^{-2} \cdot K^{-1}$ results from a thickness of 2 cm. Thus slim, yet highly insulating façade constructions can be realized. As the kernel has nano-size pores, the gaseous thermal conductivity becomes noticeable only for pressures above 10 mbar. Only above 100 mbar the thermal conductivity doubles to about $8 \times 10^{-3}\,W \cdot m^{-1} \cdot K^{-1}$, such a pressure could occur after several decades of usage in a middle European climate. These investigations revealed that the pressure increase is due to water vapor permeating the laminate itself, and to N_2 and O_2, which tend to penetrate the VIP via the sealed edges. An extremely important innovation is the integration of a thermo-sensor into the VIP to nondestructively measure the thermal performance *in situ*. A successful "self-trial" was the integration of about 100 hand-made VIPs into the new ZAE-building in Würzburg. Afterwards, several other buildings were super-insulated using

[1] Invited paper presented at the Seventh European Conference on Thermophysical Properties, September 5-8, 2005, Bratislava, Slovak Republic.

[2] Bavarian Center for Applied Energy Research e.V. (ZAE Bayern), Am Hubland, 97074 Würzburg, Germany.

[3] To whom correspondence should be addressed. E-mail: fricke@zae.uni-wuerzburg.de

VIPs within a large joint R&D project initiated and coordinated by ZAE Bayern and funded by the Bavarian Ministry of Economics in Munich. These VIPs were manufactured commercially and integrated into floorings, the gable façade of an old building under protection, the roof and the facades of a terraced house as well as into an ultra-low-energy "passive house" and the slim balustrade of a hospital. The thermal reliability of these constructions was monitored using an infrared camera.

KEY WORDS: heat transfer; thermal conductivity; thermal insulation; vacuum insulation panel (VIP).

1. INTRODUCTION

Evacuated insulations are now known for more than a century. Evacuated "Dewars" were invented by James Dewar in 1890, and "Thermos"-bottles were produced by the German company Thermos GmbH later. Such systems make use of high vacuum (pressure below 10^{-4} mbar) to suppress gaseous conduction and of highly reflecting walls (infrared emissivity typically 0.05) to reduce radiative thermal transport. They are used in cryo techniques and for domestic thermal storage and are either made of thin glass or steel envelopes. Due to their cylindrical or spherical shape, their walls are load-bearing with respect to atmospheric pressure of $10^5\,\mathrm{N}\cdot\mathrm{m}^{-2}$ (which corresponds to a load of 10 tons per m^2).

Even better insulating properties can be obtained with evacuated foil insulations [1]. Here, several highly reflecting layers of crinkled or embossed metal foil (often separated by a thin fibrous layer) or metal-coated polyimide foils are inserted into the evacuated spacing. Effective thermal conductivities of below $10^{-4}\,\mathrm{W}\cdot\mathrm{m}^{-1}\cdot\mathrm{K}^{-1}$ at room temperature can be obtained (see Fig. 1).

If one wants to transfer the Dewar idea to flat panels, a load-bearing material has to be inserted between the evacuated walls – otherwise, they would collapse. Such vacuum insulation panels (VIPs) have a history of several decades. Powder-filled VIPs were patented by L'Aire Liquide [2].

In the 1980s, Brown Boverie and Cie (BBC) in Heidelberg developed rectangular evacuated casings, filled with powders and fiber mats for the insulation of the sodium–sulphur high temperature battery [3, 4]. In the beginning of the 1990s, Degussa in Hanau manufactured VIPs with a filling of precipitated silica and a deep-drawn high-barrier plastic envelope for refrigerators [5]. At the same time, Owens Corning began to develop fiber-filled VIPs with sheet steel casing, sheets with a thickness of 75 μm [6]. At MBB not only were VIPs with a 100 μm sheet steel casing and a diatomite fill developed, but also tests with a vacuum-insulated pipe for district heating were performed [7]. In the 1990s, Dow Chemical [8] and

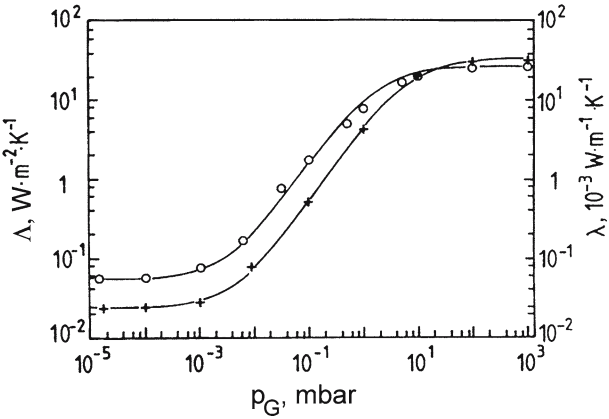

Fig. 1. Heat transfer coefficient Λ and apparent thermal conductivity λ of a 1 mm thick evacuated foil insulation at 303 K as a function of gas (air) pressure. + = 7 Al-foils 12 mm thick, separated by cellulose layers ($10\,g \cdot m^{-2}$); o = one polyimide foil (8 μm thick) on both sides coated with Al, sandwiched between glass fiber paper ($16\,g \cdot m^{-2}$) [1].

ICI [9] developed open-porous polystyrene and polyurethane foams, which were sealed into high barrier laminates. For applications in cars, BMW and Längerer and Reich developed a latent heat storage device with vacuum insulation [10]. As filling materials, silica aerogels were employed.

Nowadays, prerequisite for VIP-production is the development of flexible laminates, which provide an efficient barrier against O_2, N_2 and H_2O penetration, and, on the other side, result in negligible thermal bridging across the edges of the VIPs. Stimulation for developments in this respect arose from increasingly more stringent packaging requirements in the food, pharmaceutical, and electronics industries.

Another prerequisite was the availability of highly porous nanostructured kernels with a high thermal resistance, maintained even under a moderate pressure increase. A pioneer for nanomaterials was Kistler [11], who first made silica aerogels in the 1930s in a wet-chemical process and measured their thermal properties. He found that their thermal conductivity in air was around $0.020\,W \cdot m^{-1} \cdot K^{-1}$, i.e., considerably lower than for other insulants. He also revealed that evacuation to a pressure of 10 mbar was sufficient to suppress gaseous thermal conduction (at least for aerogel monoliths and fine aerogel powders). His measurements were repeated by our research group in the 1980s under well-defined conditions concerning the external load (Fig. 2). In principle, Kistler's data were confirmed.

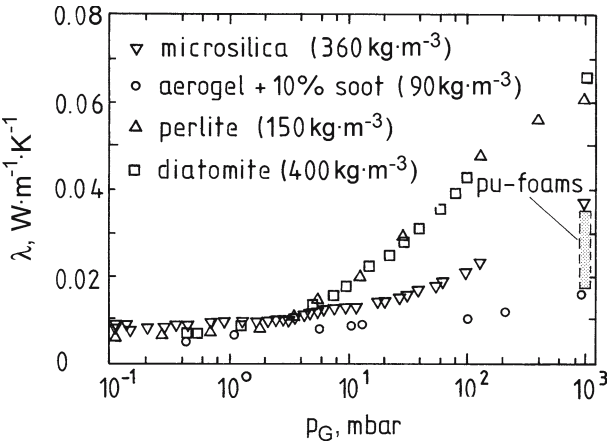

Fig. 2. Thermal conductivity of various silica powders as a function of gas (air) pressure at 300 K. External load onto the specimen is 1 bar [12]. Nanostructured silica aerogels have a lower thermal conductivity than the other powders at all gas pressures. Perlite and diatomite have conductivities above $0.060\,W \cdot m^{-1} \cdot K^{-1}$ in air. Numbers in brackets are the densities of the powders.

Although development activities for large-scale production of aerogels were pursued by several large chemical companies in the 1980s and 1990s [13, 14], silica aerogels did not become available in sufficiently large quantities.

A systematic screening of powders, fibers and foams with respect to their insulating properties at our institute in Würzburg revealed (Fig. 3) that load-bearing evacuated fibers provided the largest thermal resistance among all insulating materials, however, they showed a doubling of conductivity, once the gas pressure surpassed 1 mbar.

Contrariwise, nanostructured fumed silica – made by burning $SiCl_4$ in a hydrogen flame – has similarly low thermal conductivities in air as silica aerogels and is also the least sensitive to an increase in gas pressure. And most important, fumed silica was already a mass product, e.g., as a thickener in paints or as filler material in tires. So, fumed silica has become the material of choice, when ZAE Bayern manufactured about 100 VIPs and integrated them into the façade of its new building in Würzburg [16, 17]. In the following years, this idea was also further pursued by other institutions.

2. VIP-CONSTRUCTION

Kernels consisting of compressed fumed silica are laced with SiC or other infrared-opacifiers in order to reduce radiative transport and

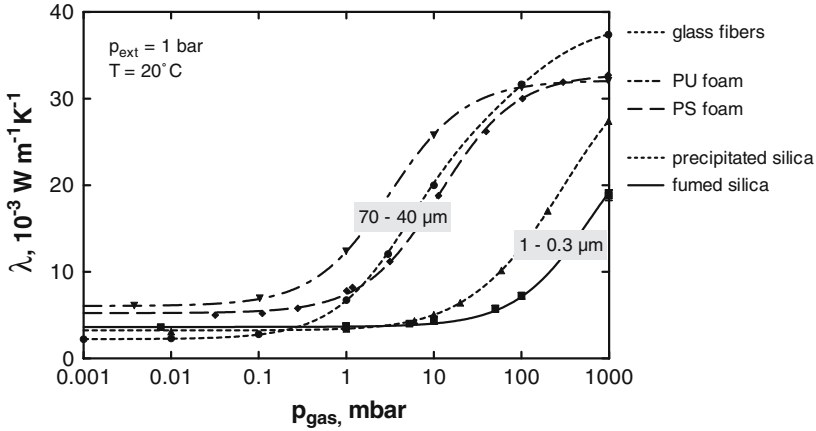

Fig. 3. Thermal conductivity of fibers, powders, and foams as a function of gas (air) pressure [15].

with organic fibers to enhance stability. The density is about 150 to $200\,\mathrm{kg}\cdot\mathrm{m}^{-3}$, which appears rather high, but is necessary to get processable boards and to prevent excessive shrinkage of more than 5% upon evacuation. The kernel is dried, evacuated to about 0.1 mbar, and sealed into a high-barrier laminate (Fig. 4).

The laminate consists of several layers of polyethyleneterephthalate (PET) or polyethylene (PE) coated with 30 nm thin Al-layers (Fig. 5). The Al-layers serve as barriers for air and water vapor. Since such thin metal layers have pin holes, commonly two or three Al-layers are integrated into the laminate. Less often almost water-tight Al-foils with a PE coating as

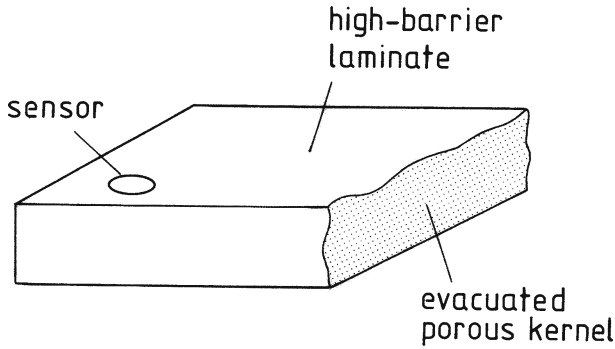

Fig. 4. Construction of a VIP with nanostructured kernel, high-barrier laminate and thermosensor.

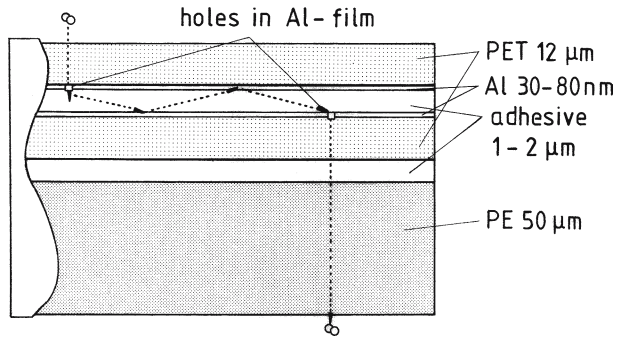

Fig. 5. Typical high-barrier laminate for VIPs.

a sealing layer are employed – the 7-μm thick Al-layer causes thermal bridging at the perimeter of the VIP.

Indispensable for quality control of the production process itself as well as for *in situ* tests of the thermal performance of the VIP on its way into a building is a thermo-sensor (Fig. 6). An especially sensitive sensor [18] uses a quasi-stationary method. Upon VIP production, a 1-mm thick metal plate (diameter about 30 mm), covered with a thin fleece layer, is sandwiched between the kernel and laminate. The fleece has a much coarser pore structure than the kernel and thus a noticeable increase in gaseous thermal conductivity occurs even for a small increase in gas pressure (while the gaseous conductivity of the kernel is still negligible). For measurements, a hot sensor head is pressed onto the sensor position. The sensor head gives off more heat, the larger the conductivity λ_F of the fleece is, i.e., the higher the gas pressure p_G is within the VIP. If the $\lambda_F(p_G)$ dependence is known from a calibration, the fumed silica curve in Fig. 3 allows one to derive the thermal conductivity λ_K of the kernel from the gas pressure p_G. Most easy is the data evaluation if the temperature of the sensor head is kept constant by integrating an electrical heater into it. The supplied electrical power $P_{el}(t)$ is measured and plotted logarithmically versus t:

$$\ln P_{el} = \text{ const.} - \xi t, \tag{1}$$

with $\xi = (\lambda_F/d_F)A_S/C_S$. Here, d_F is the thickness of the fleece, A_S is the sensor area, and C_S is the heat capacity of the sensor plate. If these three parameters are known, λ_F can be derived from ξ (the slope) in the logarithmic plot. It is noteworthy that the starting temperatures of the sensor and the sensor head need not be known.

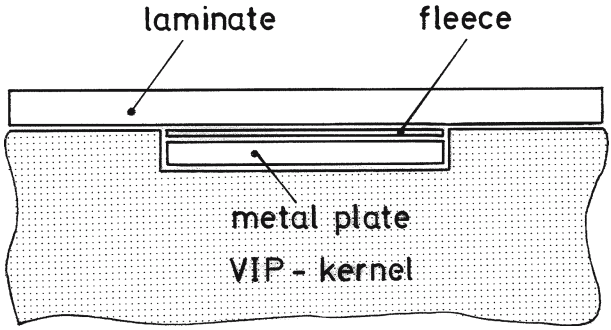

Fig. 6. "va-Q-check"-sensor, integrated into VIPs, allows early detection of gas permeation [18].

3. THERMAL TRANSPORT IN VIPs

The kernel has to be optimized with respect to the gaseous thermal conductivity λ_G, the solid thermal conductivity λ_S, and the radiative thermal conductivity λ_R, all three of which add up to the total thermal conductivity λ. Also a coupling term λ_C has to be included;

$$\lambda = \lambda_G + \lambda_S + \lambda_R + \lambda_C. \tag{2}$$

λ_C is negligible for foams with non-broken structure. Contrariwise, it can be considerable at elevated gas pressures, e.g., 0.020 to $0.030\,W \cdot m^{-1} \cdot K^{-1}$ for powders consisting of hard grains (see Fig. 2, examples, perlite and diatomite). The coupling term becomes noticeable, when – upon an increase of the gas pressure – the contact resistances between the grains are thermally shorted by the gas molecules.

The gas conductivity λ_G varies with the gas pressure p_G according to [19]

$$\lambda_G = \lambda_{G0}/(1 + 2ß Kn) = \lambda_{G0}/(1 + p_{1/2}/p_G). \tag{3}$$

$\lambda_{G0} = 0.026\,W \cdot m^{-1} \cdot K^{-1}$ is the gaseous conductivity of free still air at 300 K, ß$\approx$ 1.6 for air, $Kn = l/\Phi$ is the Knudsen number (where l is the mean free path of the gas molecules and Φ is the pore width of the porous insulant). $p_{1/2}$ is the gas pressure at which the gaseous thermal conductivity is equal to $\lambda_{G0}/2$. According to Eq. (3), we get for air,

$$p_{1/2} \approx 230\,\text{mbar}/(\Phi/\mu\text{m}). \tag{4}$$

From this equation and Fig. 7 we recognize, that for nanostructured materials with $\Phi \approx 200$ nm, one gets $p_{1/2} \approx 1000$ mbar. And if the gas pressure

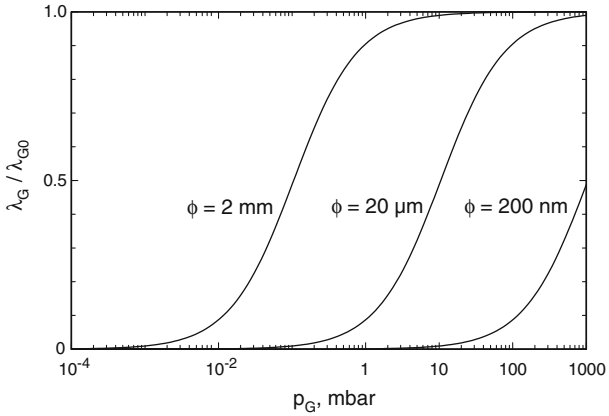

Fig. 7. Variation of the relative gaseous thermal conductivity as a function of gas (air) pressure p_G, with the pore width Φ as a parameter, temperature $T \approx 300\,\mathrm{K}$.

is reduced to below 10 mbar, the gaseous conductivity is negligible. For coarser materials with $\Phi \approx 20\,\mu\mathrm{m}$, the gaseous conductivity is fully developed at 1 bar and evacuation to about 0.1 mbar is required, in order to suppress gaseous conduction.

The solid conductivity λ_S is the smaller, the more thermal resistances are built into the insulating material, i.e., the finer structured the material is. Nano-materials are superior in this respect, as they resemble fractals, which interrupt the heat flow on the nm-level, while perlite and diatomite consist of rather coarse, well-conducting grains. The solid conductivity scales with the density ρ of the material;

$$\lambda_S \sim \rho^{\alpha}, \tag{5}$$

where $\alpha \approx 1$ for foams and $\alpha \approx 1.5\ldots2$ for materials such as aerogels or fumed silica. The solid conductivity also depends on the external pressure load onto the material; a quantitative description is difficult, as most materials show a hysteresis behavior. Typical values for pressure-loaded fibers are $\lambda_S \approx 0.001\ldots0.003\,\mathrm{W \cdot m^{-1} \cdot K^{-1}}$; for powders, $\lambda_S \approx 0.003\ldots0.010\,\mathrm{W \cdot m^{-1} \cdot K^{-1}}$; and for pressure sustaining foams, $\lambda_S \approx 0.005\,\mathrm{W \cdot m^{-1} \cdot K^{-1}}$.

In order to reduce the radiative thermal transport at a given temperature, as much absorbing and scattering particles have to be integrated into the insulating material. As silica is a weak absorber in the near infrared, an opacifier, e.g., SiC has to be added. Quantitatively the radiative thermal conductivity is described by [20]

$$\lambda_R = \frac{16n^2\sigma T_r^3}{3E(T_r)}. \tag{6}$$

Here, n is the index of refraction, which can be approximated by $n \approx 1$ for low density silica. $\sigma = 5.67 \times 10^{-8}\,W \cdot m^{-2} \cdot K^{-4}$ is the Stefan-Boltzmann constant, and T_r is an average temperature within the insulant;

$$T_r^3 = (T_1 + T_2)(T_1^2 + T_2^2)/4. \tag{7}$$

T_1 and T_2 are the temperatures of the VIP surfaces. $E(T_r)$ is the extinction coefficient of the insulating material, which is the reciprocal of the mean free path l_{ph} of the thermal photons and is correlated with the density ρ and the mass specific extinction $e(T_r)$ as follows:

$$E(T_r) = e(T_r)\rho = 1/l_{ph}. \tag{8}$$

For opacified silica kernels, one has $l_{ph} \approx 100\mu m$, which means that VIPs with a thickness of 2 cm are infrared-optically thick. $e(T_r)$ can be calculated from the spectral mass specific extinction $e(\underline{\lambda})$, which is derived from infrared-optical extinction measurements within the wavelength range $\underline{\lambda} = 2...40\mu m$ (see Fig. 8). By properly averaging $e(\underline{\lambda})$ over the diffusing thermal spectrum at T_r ("Rosseland"average), $e(T_r)$ is obtained (Fig. 9).

According to Eq. (6), typical radiative conductivities of an opacified silica kernel at $T = 300\,K$, with a mass specific extinction $e \approx 50...60\,m^2 \cdot kg^{-1}$ and a density $\rho \approx 150\,kg \cdot m^{-3}$, are $\lambda_R \approx 0.001\,W \cdot m^{-1} \cdot K^{-1}$.

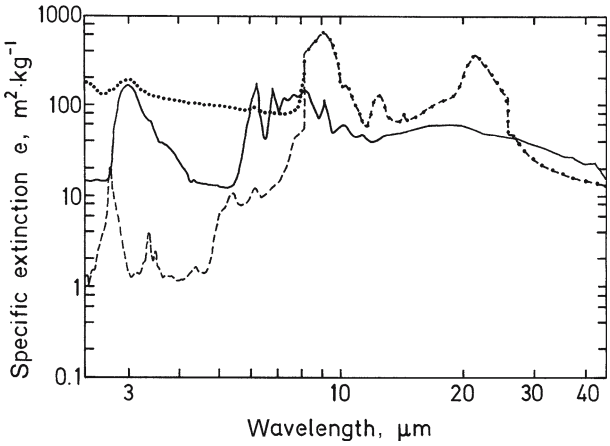

Fig. 8. Spectral mass specific extinction versus wavelength for pure silica aerogel (- - -), organic resorcinol–formaldehyde aerogel (—) and for opacified silica with 5% carbon black (... ..) [21].

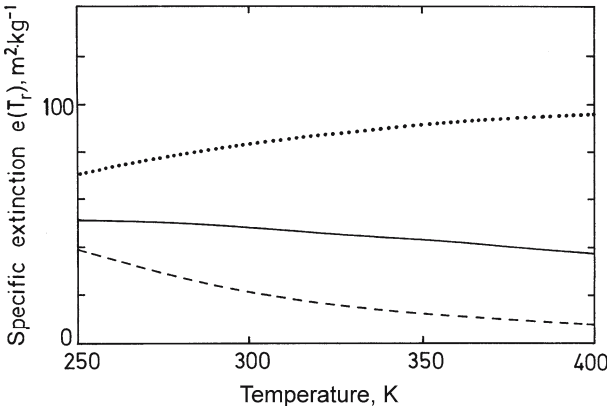

Fig. 9. Mass specific extinction as a function of temperature of the materials in Fig. 8 [20].

To wrap up the details in this section, one can expect total thermal conductivities of about $0.004\,W \cdot m^{-1} \cdot K^{-1}$ for dried and evacuated opacified silica kernels, with contributions of $0.003\,W \cdot m^{-1} \cdot K^{-1}$ from solid conduction and $0.001\,W \cdot m^{-1} \cdot K^{-1}$ from radiative transport.

4. DEGRADATION OF VIP PERFORMANCE WITH TIME

High-barrier laminates, which enclose the silica kernel and are sealed along its perimeter, are not absolutely vacuum tight. We have to consider the penetration of N_2 and O_2 into the VIP, which – as we shall see – occurs preferentially via the rim seal or point-like defects. Despite the Al-coatings (shown in Fig. 5), water permeation through the laminate itself leads to a pressure (and mass) increase with time. The pressure increase can be measured using the so-called foil lift-off method [22]: the VIP is placed into a vacuum chamber and the pressure in the chamber is gradually reduced. If the pressure in the chamber becomes smaller than the pressure within the VIP, the VIP-cover lifts off the kernel, which can be recorded with a photoelectric sensor. The mass increase with time can be determined by repeated weighing.

We have measured the pressure and the mass increase for fumed silica VIPs sized at $10\,cm \times 10\,cm \times 1\,cm$ and at $20\,cm \times 20\,cm \times 1\,cm$. Three different laminate types were employed. The VIPs were stored in air-conditioned boxes over a period of about 1 year. In a dry climate, linear increases of pressure with time are observed (Fig. 10). (The linear increases should proceed for much longer times, as long as the pressure

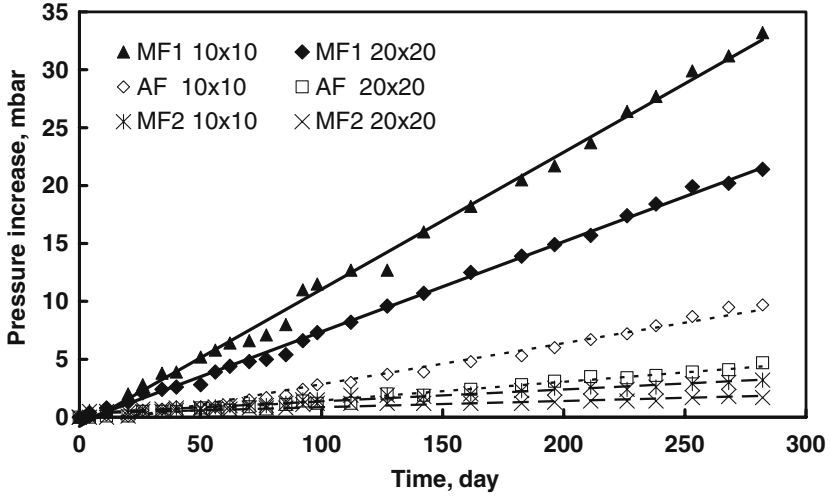

Fig. 10. Measured pressure increases over time for fumed silica VIPs of different sizes stored in climate chambers at 45°C and a water vapor pressure of 14 mbar, which corresponds to a relative humidity of 15%. Envelope types were one Al-foil laminated with PE (AF) and two Al-coated multilayer laminates (MF) [22].

inside the VIP is much smaller than atmospheric pressure.) The increases are quite different for the three envelope types. For the larger VIPs with doubled circumference (i.e., rim seal length) and quadrupled volume for the relatively tight laminates AF and MF2, only one half of the pressure increase is detected. This indicates that the pressure increase is mainly caused by a length related leakage, i.e., gas infusion via the rim seal. Also, a strong dependence of the leakage rates on temperature was observed (not shown here), which can be explained by a thermally activated diffusion process and described by an Arrhenius law.

Another set of VIPs was stored in boxes with a moist climate. The data from weighing are depicted in Fig. 11. Linear increases in mass with time are observed. (We should note, that for very long times the mass increase has to level off, because the driving force for the water infusion is the difference between the vapor pressure outside and inside. For moist VIP kernels, which were stored in a dry climate, even a mass decrease was observed.) Quite different mass increases occur for the different types of envelopes. From the size dependence of the mass increases, one can conclude that the water vapor enters the VIP preferentially via the laminate itself.

The water, which has penetrated the VIP envelope, leads to a vapor pressure build-up, which is determined by the sorption isotherm of the kernel material (Fig. 12). A water content of 1% by mass thus leads to

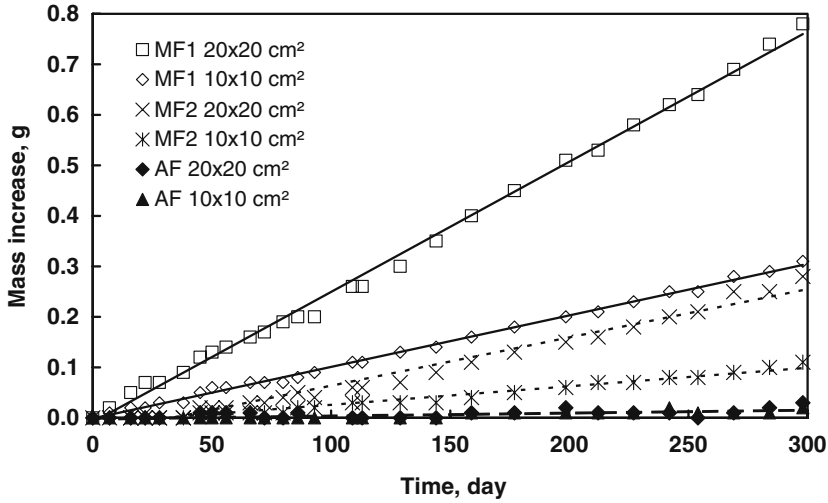

Fig. 11. Measured mass increases over time for fumed silica VIPs of different sizes stored in climate chambers at 25°C and a water vapor pressure of 24 mbar, which corresponds to a relative humidity of 75%. Envelopes were of the same type as in Fig. 10 [22].

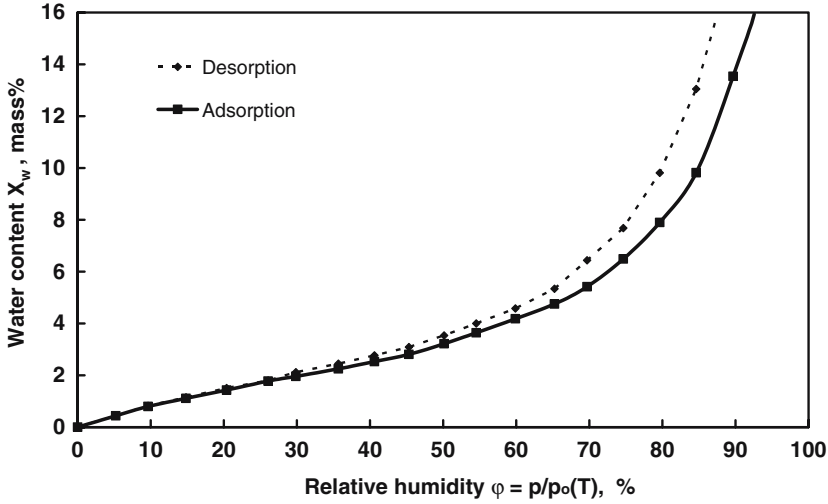

Fig. 12. Sorption isotherms for fumed silica kernels at 23°C. Plotted is the water content in mass% of the dry kernel versus the relative vapor pressure [22].

a relative humidity of about 10%, which corresponds to a water vapor pressure of 2.3 mbar at 20°C. The gaseous thermal conductivity of free water vapor is $0.016\,W \cdot m^{-1} \cdot K^{-1}$ and the characteristic pressure $p_{1/2} \approx 120\,\text{mbar}/\Phi/\mu\text{m})$. From these data, the dependence of the gaseous thermal conductivity of water vapor in a fumed silica kernel, shown in Fig. 13, can be calculated.

Both air and water vapor within the kernel contribute to the thermal conductivity. Our investigations showed that for a typical middle European climate and the best available laminates a pressure increase of less than 1 mbar per year can be achieved. According to Fig. 3, the thermal conductivity thus remains below about $0.006\,W \cdot m^{-1} \cdot K^{-1}$ within a time span of 50 years, typical for building applications. We also found that a maximal water content of 3–7 mass% can be expected in building applications in a typical middle European climate [23]. This would lead to a maximal vapor pressure of about 15 mbar, corresponding to an additional water vapor induced gaseous thermal conductivity of less than $0.002\,W \cdot m^{-1} \cdot K^{-1}$ (see Fig. 13). Overall, the thermal conductivity of the VIP thus is expected to remain below $0.008\,W \cdot m^{-1} \cdot K^{-1}$ even after 50 years of usage.

An effect, which we only want to mention here, is the sudden displacement of adsorbed water within the VIP kernel if, e. g., the warm and cold sides of a VIP are interchanged, or more general, if non-

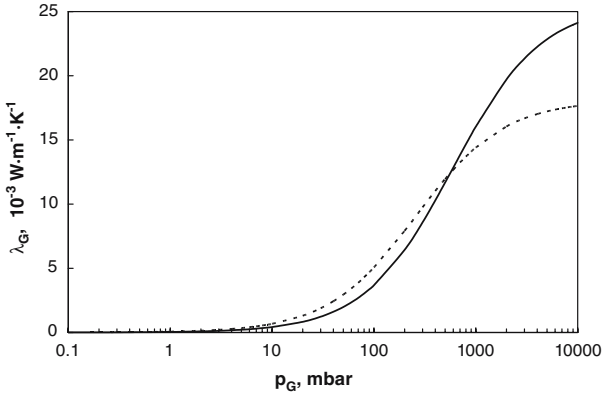

Fig. 13. Measured gaseous thermal conductivity of air (—) and calculated gaseous thermal conductivity of water vapor (...) within a fumed silica kernel. Water vapor has a smaller $p_{1/2}$-value than air, but a smaller λ_{G0}-value, thus the two curves show a cross-over. Due to condensation of water vapor above about 20 mbar within the nanoporous silica, only part of the $\lambda_G(p_G)$-curve is valid.

stationary conditions are prevalent. The water displacement is correlated with a significant transfer of latent heat within the kernel. Another effect, which is not discussed here, is the increase in solid thermal conduction by the adsorbed water.

5. APPLICATIONS

VIPs have had a successful start in domestic appliances as well as in the logistics area, where longtime temperature constancy is required. One example of the latter is a passive transport container insulated with VIPs [24]. Measuring 1.4 m × 1.1 m × 1.6 m, this container can maintain a temperature of – 18°C for 4 days or stay within a temperature span of +2°C to +8°C for 9 days. To increase the heat capacity of the system, phase change materials are loaded into the container.

Building-related applications, which were pursued by ZAE Bayern, are the integration of VIPs into floorings, facades, roofs, and slim balustrades (see Figs. 14 through 17). Even an ultra-low energy house ("Passive House") was realized, using VIPs [25]. Details can be found at www.vip-bau.de.

6. OUTLOOK

Without the tremendous progress in the quality of high-barrier laminates, long-time applications of VIPs in building technology would not be

Fig. 14. In 1998 first installation of VIPs in a building at the test façade of ZAE Bayern. For testing purposes VIPs were integrated into the spacing of a jamb-crossbar construction.

Fig. 15. Gable façade of an old building under protection during the installation (left) and after renovation was finished (right). The shiny VIPs are in a rail system. The pale pink polystyrene boards have just been mounted.

Fig. 16. Photograph (left) of the new ultra-low energy timber building and the infrared image (right) of the VIP insulated building envelope (architect: F. Lichtblau/Munich, Germany).

possible. Also, the progress in understanding the thermal transport in VIPs and the influence of gas and moisture intake as well as stringent quality control and the availability of simple and fast sensors have strengthened the confidence in the VIP as a technical innovation.

A to-do list for the future remains: develop even better laminates, which allow the use of cheaper kernel materials; develop an RFID sensor, which can be read out without requiring direct thermal contact with the VIP surface; and keep promoting the integration of VIPs into insulation systems for protection and simpler application in the building process.

Fig. 17. Jamb-crossbar construction made of aluminum: vacuum-insulated facade-elements during the installation (left) and outside view of the façade (right).

REFERENCES

1. K. G. Degen, S. Rossetto, R. Caps, and J. Fricke, *Thermal Conductivity* **22**, T. W. Tong, ed. (Technomic Publ. Co. Inc., Lancaster/Basel, 1994), pp. 401–412.
2. P. P. Gervais and D. Goumy, *Insulating Material with Low Thermal Conductivity, formed of a Compacted Granular Structure*, US-Patent 4,159,359 (June 26, 1979).
3. W. Fischer and W. Haar, *Physik in unserer Zeit* **9:**184 (1978).
4. R. Caps, J. Fricke, and H. Reis, *High Temps. – High Press.* **15**:225 (1983).
5. R. Reuter and G. Sextl, Degussa AG, Hanau, "Vacuum Insulation Panels (VIPs)," at *1993 Non-Fluorocarbon Insulation, Refrig. and Air-Conditioning Technol. Workshop*, Wiesbaden (1993).
6. R. McGrath, Owens Corning, ibid.
7. L. Schilf, MBB, The MBB-Vacuum Super Insulation (VSI), ibid.
8. P. Pendergast and B. Malone, *Vuoto scienza et tecnologia*, Vol. XXVIII, No. 1–2:77 (1999).
9. A. J. Hamilton, *Vuoto scienza et tecnologia*, Vol. XXVIII, No. 1–2:27 (1999).
10. P. Blüher, *ATZ Automobiltechnische Zeitschrift* **93**, Heft 10 (1991).
11. S. S. Kistler, *J. Phys. Chem.* **34**:52 (1932).
12. J. Fricke, M. C. Arduini-Schuster, D. Büttner, H.-P. Ebert, U. Heinemann, J. Hetfleisch, E. Hümmer, J. Kuhn, and X. Lu, "Opaque Silica Aerogel Insulations as Substitutes for Polyurethane (PU) Foams," *21st Int. Thermal Conductivity Conf.*, Lexington, Kentucky (1989).
13. G. Herrmann, R. Iden, M. Mielke, F. Teich, and B. Ziegler, *Non-Cryst. Solids* **186**:380 (1995).
14. "Innovative Heat Insulation with Aerogels," Hoechst AG, Frankfurt VF1255–1-2 e/0507(014), in *Future Special Science* **2** (1997).
15. *ZAE-Data*, U. Heinemann (2002), ZAE Bayern, Am Hubland 97074, Germany (www.vip-bau.de/technology.htm).
16. M. Volz and S. Wolf, *DBZ Heft* **1**:46 (2000).
17. R. Caps, U. Heinemann, and J. Fricke "Application of Vacuum Insulations in Buildings," presented at *Vacuum Insulation Association Symp.* "*Progress in Vacuum Insulation*," Vancouver (2000).

18. R. Caps, "Vorrichtung und Verfahren zur Messung des Gasdruckes in evakuierten Dämmplatten," *Patent DE 10215213C1* (2002).
19. M. G. Kaganer, *Thermal Insulation in Cryogenic Engineering* (Israel Program for Scientific Translations, Jerusalem, 1969).
20. J. Fricke, *High Temps. – High Press*. **25**:379 (1993).
21. X. Lu, M. C. Arduini-Schuster, J. Kuhn, O. Nilsson, J. Fricke, and R. W. Pekala, *Science* **225**:971 (1992).
22. H. Schwab, U. Heinemann, A. Beck, H.-P. Ebert, and J. Fricke, *J. Thermal Env. Bldg. Sci.* **28**:293 (2005).
23. H. Schwab, U. Heinemann, J. Wachtel, H.-P. Ebert, and J. Fricke, *J. Thermal Env. Bldg. Sci.* **28**:327 (2005).
24. *va-Q-tec AG*, Würzburg.
25. *www.vip-bau.de*.